

PAPER • OPEN ACCESS

On quantum reliability characterizing systematic errors in quantum sensing

To cite this article: Lian-Xiang Cui *et al* 2025 *J. Reliab. Sci. Eng.* **1** 015004

View the [article online](#) for updates and enhancements.

You may also like

- [Probabilistic calibration of model parameters with approximate Bayesian quadrature and active machine learning](#)
Pengfei Wei, Masaru Kitahara, Matthias G R Faes et al.
- [Adaptive artificial neural network for uncertainty propagation](#)
Yan Shi, Lizhi Niu and Michael Beer
- [Detecting and eliminating quantum noise of quantum measurements](#)
Shuanghong Tang, Congcong Zheng and Kun Wang

On quantum reliability characterizing systematic errors in quantum sensing

Lian-Xiang Cui (崔廉相)¹, Yi-Mu Du (杜亦牧)^{2,*}
and Chang-Pu Sun (孙昌璞)^{2,1,*}

¹ Beijing Computational Science Research Center, Beijing 100193, People's Republic of China

² Graduate School of CAEP, Beijing 100193, People's Republic of China

E-mail: ymdu@gscaep.ac.cn and suncp@gscaep.ac.cn

Received 13 November 2024, revised 5 January 2025

Accepted for publication 6 January 2025

Published 24 January 2025



Abstract

Quantum sensing utilizes quantum effects, such as entanglement and coherence, to measure physical signals. The performance of a sensing process is characterized by error which requires comparison to a true value. However, in practice, such a true value might be inaccessible. In this study, we utilize quantum reliability as a metric to evaluate quantum sensor's performance based solely on the apparatus itself, without any prior knowledge of the true value. We derive a general relationship among reliability, sensitivity, and systematic error, and demonstrate this relationship using a typical quantum sensing process. That is to measure magnetic fields (as a signal) by a spin-1/2 particle and using the Stern–Gerlach apparatus to read out the signal information. Our findings illustrate the application of quantum reliability in quantum sensing, opening new perspectives for reliability analysis in quantum systems.

Keywords: quantum reliability theory, reliability analysis, error analysis, reliability of quantum sensor, reliability of measurement apparatus

1. Introduction

A sensor's functioning highly relies on its measurement process, which converts observations into numbers to quantify the phenomena, thereby shaping the depth and clarity of our understanding of the world. The reliability of these measuring apparatus plays a pivotal role. The readings of any apparatus usually consist of the true value of the measured signal and the error introduced during the measurement process [1], with the performance of the apparatus highly related to these two factors. The discourse on measurement errors holds profound significance across various fields. From the physiological data of patients in medicine [2, 3] to the experimental

data in biochemistry laboratories [4], from the minutiae of atomic frequency [5] to the grand detection of gravitational waves in the cosmos [6, 7], the accuracy of measurement is of utmost importance. Meanwhile, the field of reliability engineering also places significant emphasis on the measurement of errors [8–12].

Recently, quantum sensing, as a new technology on highly precise measurements, is widely concerned [5, 13–15]. It encompasses the utilization of quantum systems or effects to measure physical quantities, whether they be classical or quantum, such as electromagnetic fields, time or frequency, temperature, and pressure. Quantum measurement apparatus exploit a key characteristic of quantum systems: their heightened sensitivity to external perturbations, which enables highly precise measurements. Additionally, intrinsic quantum properties like coherence and entanglement [16–18] are harnessed to perform these measurements. Many quantum measurement apparatus have already been integrated into our daily lives, including nuclear magnetic resonance [19–22] and atomic clocks [23].

* Author to whom any correspondence should be addressed.



Original Content from this work may be used under the terms of the [Creative Commons Attribution 4.0 licence](https://creativecommons.org/licenses/by/4.0/). Any further distribution of this work must maintain attribution to the author(s) and the title of the work, journal citation and DOI.

A fundamental aspect of evaluating the performance of a measurement apparatus is the assessment of error. Typically, assessing the systematic error of such an apparatus requires a true value of the measured quantity for comparison. This true value is ideally provided by a ‘yardstick’—a perfectly standard apparatus. However, when the true value is inaccessible, an alternative metric must be identified to characterize the apparatus’s performance. In such cases, reliability emerges as a crucial indicator.

Reliability measures an apparatus’s ability to consistently perform its function. It is determined by the performance of each component in the system; as long as each step operates as designed, the output remains reliable. Importantly, in measurement processes, reliability is intrinsic to the apparatus and does not depend on the true value being measured. Unlike error, which focuses on the outcome, reliability takes a reductionist approach by evaluating the quality of each individual step in the process. Thus, while error is concerned with results, reliability concentrates on the process.

In the current study, we characterize the measurement error by reliability. A relationship among reliability, sensitivity, and systematic error of measurement apparatus is derived, showing that when the apparatus is near ideal, there is a proportional relationship between the decrease in reliability and the sensitivity times systematic error, i.e.

$$1 - \text{Reliability} \propto \text{Sensitivity} \times \text{Error}. \quad (1)$$

Here, the proportionality coefficient is determined solely by the measuring apparatus and is independent of the physical quantity being measured. From this relationship, we can infer the systematic error of the apparatus through its reliability, thereby eliminating the need for a standard reference scale. We then focus on the quantum sensing process, using a typical quantum sensing model to illustrate this relationship: sensing a magnetic field via spin and employing the Stern–Gerlach (SG) apparatus to measure the spin state.

This paper is structured as follows. Section 2 provides a brief introduction to the concepts of measurement error and derives the relationship among reliability, sensitivity, and systematic error. Section 3 explores sensing and reliability within the quantum scheme. Section 4 illustrates the relationship discussed in section 2 through a specific quantum sensing process. Finally, section 5 summarizes our findings and suggests directions for future research.

2. Measurement error and reliability

Measurement is the process of converting a physical quantity into a numerical reading. This conversion can be direct, such as determining length using a ruler, or indirect, such as transforming a signal into a reading via sensors. Here, we refer to the entire progression from the physical quantity to its numerical representation as the measurement process, which is the focus of our study in this paper. Before commencing our discussion, it is essential to define measurement errors clearly. This section specifically delineates systematic and random

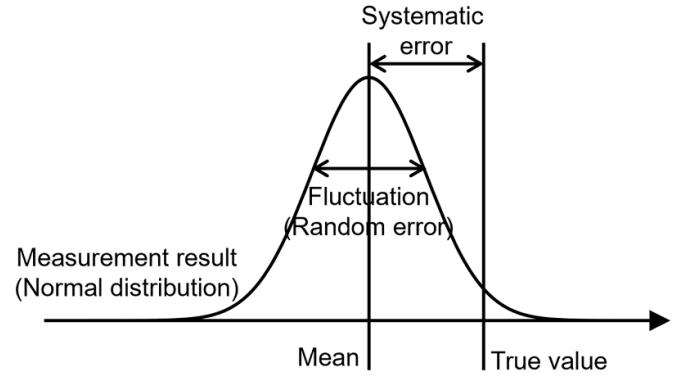


Figure 1. Schematic representation of measurement error.

errors and derives the relationship among the reliability, sensitivity, and systematic errors of measuring apparatus.

2.1. Measurement error

Measurement has long been a topic of significant concern. When describing measurements, it is imperative to carefully define the terminology used to ensure a common foundational basis for discussion. Numerous international organizations, including the Bureau International des Poids et Mesures (BIPM), the International Electrotechnical Commission (IEC), the International Organization for Standardization (ISO), and the International Organization of Legal Metrology (OIML), etc have come together to publish manuals that precisely define these terms, International Vocabulary of Metrology (VIM) [24] and Guide to the Expression of Uncertainty in Measurement (GUM) [25].

Here, we focus on measurement error, a measured quantity value minus a reference quantity value (true value). Measurement errors are traditionally categorized into two types: random errors and systematic errors [4]. Let x represent the true value of the measurand and \hat{x} the observed measurement. The observed measurement can then be expressed as the sum of the true value x , random error ϵ , and systematic error δ , i.e.

$$\hat{x} = x + \epsilon + \delta. \quad (2)$$

Random error ϵ refers to the error that in replicate measurements varies unpredictably. The results of multiple measurements typically yield a distribution, which, under normal circumstances, follows a Gaussian distribution. The width of this Gaussian distribution, characterized by its variance (fluctuations), is attributed to random noise. In contrast, the deviation of the mean of this distribution from the true value is due to systematic error δ , as illustrated in figure 1.

It is important to note that the aforementioned errors rely on a true value, which serves as a reference quantity. In the absence of access to this true value in practical scenarios, does this imply an inability to assess the apparatus’s quality? In the subsequent discussion, we will evaluate the reliability of the measurement apparatus to ascertain the accuracy of its readings. Specifically, if the apparatus operates as designed, i.e. it operates reliably, its readings should be accurate.

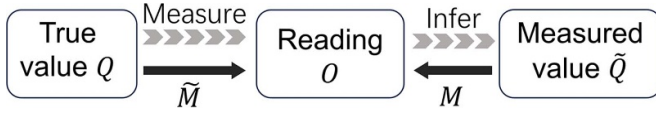


Figure 2. Diagrammatic description of definitions.

2.2. Reliability, sensitivity and systematic error

Reliability is defined as the probability that a product, system, or service will perform its intended function adequately for a specified period of time, or will operate in a defined environment without failure [26]. The function of a measurement apparatus is to provide accurate values corresponding to the measurand. Therefore, we can assess the magnitude of an apparatus's error by evaluating its reliability.

Reliability can be determined by a set of intrinsic parameters that are independent of external information. However, in the context of measurement apparatus, an intriguing question arises: what is the relationship between their reliability and measurement errors? Here, we present an analysis of the relationship among reliability, sensitivity, and systematic errors of measurement apparatus, as shown in equation (1). This relationship holds when the apparatus is nearly ideal, whether in classical or quantum systems. However, in quantum systems, the definition of reliability differs, as detailed in section 3.

To derive the aforementioned relationship, we denote the true value of the physical quantity to be measured as Q , and the reading obtained from the measurement apparatus as O . Denote the measured value of the target physical quantity, derived from the apparatus reading, as \tilde{Q} . We define two mappings here. The first one is the mapping \tilde{M} , from the true value of the physical quantity Q to the reading of the measurement apparatus O , i.e. $\tilde{M}(Q) = O$. The second one is the mapping M , from the measured value \tilde{Q} to the reading O , i.e. $M(\tilde{Q}) = O$. The definitions are illustrated in figure 2.

The sensitivity S of the measurement apparatus is defined as the variation in the apparatus's reading in response to a change in the signal being measured, expressed as follows:

$$S \equiv \frac{d\tilde{M}}{dQ}. \quad (3)$$

The systematic error is defined as

$$\delta Q = \tilde{Q} - Q, \quad (4)$$

the difference of the measured value \tilde{Q} and the true value Q .

When the apparatus operation is nearly perfect, there exists a small discrepancy between real and ideal measurement processes. The linear perturbation implies that an arbitrary metrics on reliability R (where the reliability of the ideal system is normalized to 1) that quantifies this discrepancy $1 - R$, should be proportional to measurement variation $\delta M(Q)$. Formally, this relationship is given by:

$$1 - R \propto \delta M(Q). \quad (5)$$

The variation $\delta M(Q)$ can be expressed through a series expansion as:

$$\delta M(Q) = \frac{dM}{dQ} \delta Q + \frac{1}{2} \frac{d^2 M}{dQ^2} \delta^2 Q + \dots \quad (6)$$

When the first-order term is predominant, we obtain the simplified relation:

$$1 - R \propto \frac{dM}{dQ} \delta Q. \quad (7)$$

Applying definitions of sensitivity and error, this leads to the relationship found in equation (1).

In section 4, we will validate this relationship through a quantum sensing model. However, it is essential that we first clarify certain quantum concepts, which will be addressed in the following section.

3. Quantum sensing and quantum reliability

In the quantum realm, the concepts of measurement and reliability both differ significantly from those in the classical context. In quantum mechanics, quantum measurement generally refers to the measurement of quantum states. The comprehensive process we discussed earlier is known as quantum sensing, which will be the focus of our analysis. In this section, we will explore the concepts of quantum sensing and quantum reliability in detail.

3.1. Quantum sensing

Quantum sensing refers to the use of quantum systems or quantum effects to assess physical quantities (classical or quantum) [5]. However, due to the unique characteristics of quantum mechanics—such as the Born rule and the inherent uncertainty principle—it is often infeasible to directly measure the physical quantities of interest. A quantum sensing process generally encompasses several fundamental stages: the initialization of the quantum sensor, its interaction with the signal of interest, and the readout of the final state.

A quantum sensor is a discrete energy level system, typically modeled as a two-level system [27]. Quantum sensing involves inferring the properties of a target signal by examining its impact on the sensor. The procedure is as follows: initially, the sensor is prepared in a specified initial state and interacts with the target signal over a designated period. Subsequently, the quantum state of the sensor is entangled with the measurement basis, a step commonly known as quantum premeasurement. Projective measurements are then performed to the measurement basis, which often requires either repeating the process multiple times or averaging over an ensemble to determine the state. These readings allow for the inference of the target signal's characteristics. The entire process is illustrated in figure 3, with further details in [5].

In contrast to classical measurement, quantum sensing processes are inherently complex, with each step introducing potential errors. Consequently, assessing the reliability

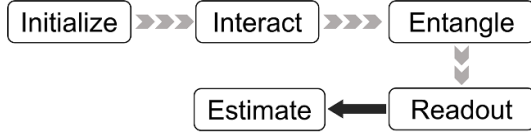


Figure 3. Schematic diagram of the quantum measurement process. The initial four steps are quantum processes, represented by grey separated arrows. The final step involves the estimation of the signal of interest through readout, which is a classical process, depicted by black arrows.

of quantum sensing necessitates careful consideration of the operational details at every stage. In this context, employing a process metric to characterize the overall system reliability offers more comprehensive insights than merely comparing result discrepancies. This approach facilitates a more precise discussion of errors. Quantum reliability, as a process metric, accurately describes whether the system's state evolves according to the intended design at each step. In the following, we introduce the concept of quantum reliability.

3.2. Quantum reliability

Quantum reliability, introduced by Cui *et al* [28], provides a novel metric for assessing the reliability of a quantum system. They define the reliable state of quantum systems and quantify the probability of reliable evolution through the consistent quantum theory [29], a measure termed as quantum reliability. We briefly introduce the concepts here.

The state of a quantum system is described by a wave function $|\psi\rangle \in \mathcal{H}$, where \mathcal{H} is the state space of the system, known as the Hilbert space. The properties of the system can be characterized using projection operators E within this Hilbert space. If the state $|\psi\rangle$ resides in the subspace \mathcal{E} corresponding to E , i.e. $E|\psi\rangle = |\psi\rangle$, then we say that the state $|\psi\rangle$ possesses the property E . Analogous to the way that the reliability of a classical system can be described by an indicator, the reliability of a quantum system can be characterized by a projector. This allows us to determine whether a quantum system is in a reliable state.

In the preceding analysis, the reliable state of a quantum system is defined. System reliability is inherently a dynamic process. To characterize the system as reliable over a given time interval, the system must maintain its reliable state throughout that interval. Only then can the system's lifetime be defined. The system may undergo a variety of evolutionary processes from time t_1 to t_n , such as reliable \rightarrow unreliable \rightarrow reliable $\rightarrow \dots$ reliable. Such a sequence of states is denoted as the system's history $\mathcal{Y} = E_1 \otimes E_2^\perp \otimes E_3 \otimes \dots \otimes E_n$, where E^\perp is the failure projection of the system and the subscript denotes time. One can define the weight of this history as

$$W(\mathcal{Y}) = \text{Tr} \left[E_n U_n \dots E_2^\perp U_2 E_1 U_1 |\psi_0\rangle\langle\psi_0| \times U_1^\dagger E_1 U_2^\dagger E_2^\perp \dots U_n^\dagger E_n \right], \quad (8)$$

where $|\psi_0\rangle$ is the initial state of the system, U_i is the evolution operator from time t_{i-1} to t_i , and U^\dagger is the Hermitian conjugate of U . To note that the weights associated with these histories do not represent their probabilities. We will subsequently discuss the conditions under which these weights can be interpreted as probabilities.

In reliability analysis, our primary concern is identifying when the system fails; the state of the system after failure is not of interest. Consequently, the histories we are interested in can be represented by the following family Θ :

$$\begin{aligned} \mathcal{F}_1 &= |\psi_0\rangle\langle\psi_0| \otimes E_1^\perp \otimes I \otimes \dots \otimes I \\ \mathcal{F}_2 &= |\psi_0\rangle\langle\psi_0| \otimes E_1 \otimes E_2^\perp \otimes I \otimes \dots \otimes I \\ &\vdots \\ \mathcal{F}_n &= |\psi_0\rangle\langle\psi_0| \otimes E_1 \otimes E_2 \otimes \dots \otimes E_{n-1} \otimes E_n^\perp \\ \mathcal{R}_n &= |\psi_0\rangle\langle\psi_0| \otimes E_1 \otimes E_2 \otimes \dots \otimes E_{n-1} \otimes E_n. \end{aligned} \quad (9)$$

Here, I is the identity, \mathcal{F}_i are the failure histories and \mathcal{R}_n is the survival history.

Define the inner product of two histories as

$$\langle \mathcal{Y}^\alpha, \mathcal{Y}^\beta \rangle \equiv \text{Tr} \left[Y_n^\alpha U_n Y_{n-1}^\alpha \dots Y_2^\alpha U_2 Y_1^\alpha U_1 |\psi_0\rangle\langle\psi_0| \times U_1^\dagger Y_1^\beta U_2^\dagger Y_2^\beta \dots U_n^\dagger Y_n^\beta \right], \quad (10)$$

where $\mathcal{Y}^k = |\psi_0\rangle\langle\psi_0| \otimes Y_1^k \otimes Y_2^k \otimes \dots \otimes Y_n^k$, $k = \alpha, \beta$. One can see that, the weight of a history \mathcal{Y} is $W(\mathcal{Y}) = \langle \mathcal{Y}, \mathcal{Y} \rangle$. When the given family satisfies the consistency condition [29, 30], the weights of the histories can be interpreted as the probabilities of these histories. The consistency condition reads: In a given family Θ , if the inner product of any two distinct histories is zero, then the family is consistent, i.e.

$$\langle \mathcal{Y}^\alpha, \mathcal{Y}^\beta \rangle = 0 \text{ for } \forall \mathcal{Y}^\alpha \neq \mathcal{Y}^\beta \in \Theta. \quad (11)$$

Thus, the reliability of a quantum system at time t_n as the probability of its survival history, denoted $R(t_n) = W(\mathcal{R}_n)$. The probability that the system has a lifetime of t_k is given by $W(\mathcal{F}_k)$, i.e. the probability that the system fails until time t_k .

Recalling figure 3, one could define quantum reliability with setting E_1 and E_2 after the 'interact' and the 'Entangle' step, receptively. The former is to check whether the signal has been successfully encoding into the sensor's state and the latter is to check whether the encoded state has been successfully correlated with the measurement apparatus's pointer state.

4. Measuring magnetic field strength with SG apparatus

In this section, we demonstrate the relationship outlined in equation (1) through a quantum sensing process, utilizing a spin-1/2 particle and a SG apparatus to detect a magnetic field. Here, the spin-1/2 particle acts as a quantum sensor, with its energy level configuration being modified upon interaction

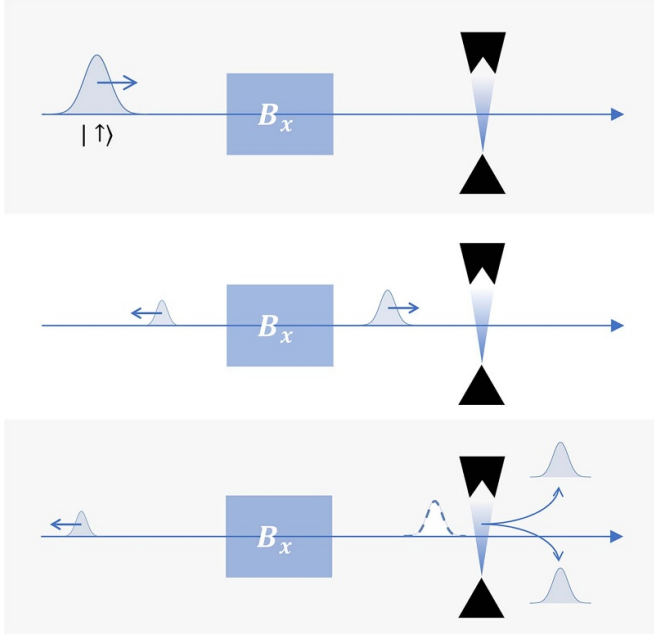


Figure 4. Schematic diagram of the quantum sensing process under consideration.

with the target magnetic field. Specifically, consider a spin-1/2 particle initially in the +1 eigenstate of σ_z , denoted as $|\uparrow\rangle$. This particle passes through a magnetic field B_x oriented along the x -direction, causing the spin to precess. A SG apparatus is then employed to measure the populations of the spin-up and spin-down states. From these measurements, the magnitude of the magnetic field can be inferred. The schematic diagram of this setup is shown in figure 4.

4.1. Ideal process

The initial momentum of the spin is $k_0 > 0$, and the width of the magnetic field to be measured is a . The evolution of the spin within the magnetic field is governed by the Hamiltonian $H_0 = B_x \sigma_x$, where σ_x is the Pauli-X matrix. After a time $t_1 = am/k_0$, the spin state evolves into

$$\begin{aligned} |\psi(t)\rangle &= e^{-iH_0 t_1/\hbar} |\uparrow\rangle \\ &= \cos \frac{B_x a m}{k_0 \hbar} |\uparrow\rangle - i \sin \frac{B_x a m}{k_0 \hbar} |\downarrow\rangle, \end{aligned} \quad (12)$$

where m is the mass of spin. The population of spin-up and spin-down are

$$\alpha = \cos^2 \frac{B_x a m}{k_0 \hbar} \text{ and } \beta = \sin^2 \frac{B_x a m}{k_0 \hbar}, \quad (13)$$

respectively. From this, the magnitude of the magnetic field to be measured can be determined through

$$B_x = \frac{k_0 \hbar}{a m} \arctan \sqrt{\frac{\beta}{\alpha}}. \quad (14)$$

4.2. Real evolution

However, in a realistic physical scenario, the incidence of spins into the magnetic field induces scattering, and the SG apparatus cannot perfectly separate the spin-up and spin-down states. This inevitably introduces systematic errors into the measurement. The real Hamiltonian writes

$$H = \frac{p^2}{2m} + \Sigma_1(\mathbf{r}) B_x \sigma_x - \Sigma_2(\mathbf{r}) B(z) \sigma_z, \quad (15)$$

where Σ_1 and Σ_2 are indicator functions that describe the regions influenced by the magnetic field and the SG apparatus, respectively. And σ_x and σ_z are Pauli-X and Z operator, respectively.

The initial state in both the x and z directions is a Gaussian wave packet with momentum k_0 along $+x$ direction, and the initial state of the spin is the +1 eigenstate $|\uparrow\rangle$ of σ_z . The total initial state writes

$$|\Psi_0\rangle = |\uparrow\rangle \otimes |\psi_{x0}\rangle \otimes |\psi_{z0}\rangle, \quad (16)$$

where

$$\begin{aligned} \psi_{x0}(x) &= \langle x | \psi_{x0} \rangle = \left(\frac{1}{2\pi\sigma^2} \right)^{1/4} e^{ik_0(x-x_0) - \left(\frac{x-x_0}{2\sigma} \right)^2}, \\ \langle z | \psi_{z0} \rangle &= \left(\frac{1}{2\pi\sigma^2} \right)^{1/4} \exp \left[-\left(\frac{z}{2\sigma} \right)^2 \right]. \end{aligned} \quad (17)$$

Here x_0 and σ are the initial position and width of the wave packet, respectively.

Following the analysis framework for quantum reliability, we first define reliable projections. For the region of the target magnetic field, reliability indicates that the spin passes through the field without reflection, achieving complete transmission. The corresponding projection operator is expressed as:

$$E_1 = \int_a^\infty I_s \otimes |x\rangle\langle x| \otimes I_z dx, \quad (18)$$

where I_s and I_z are identities in spin space and position- z space, respectively. For the SG apparatus, reliability signifies the complete spatial separation of spin-up and spin-down components along the z -axis, represented by the projection

$$\begin{aligned} E_2 &= |\uparrow\rangle\langle\uparrow| \otimes \int_b^\infty |x\rangle\langle x| dx \otimes \int_0^\infty |z\rangle\langle z| dz \\ &+ |\downarrow\rangle\langle\downarrow| \otimes \int_b^\infty |x\rangle\langle x| dx \otimes \int_{-\infty}^0 |z\rangle\langle z| dz, \end{aligned} \quad (19)$$

where b is the length of the SG apparatus in x -direction. Sometimes, the overlap integral between the spatially separated upper and lower wave packets is used to characterize the effectiveness of a SG experiment. The definition of E_2 we employ here is equivalent to the description using the overlap integral, as detailed in the derivation provided in appendix A.

Disregarding the multiple reflections of the wave packet, the family formed by these projectors is consistent. The reliability of the system writes

$$R = \text{Tr} \left[E_2 U_2 E_1 U_1 |\Psi_0\rangle \langle \Psi_0| U_1^\dagger E_1 U_2^\dagger E_2 \right], \quad (20)$$

where U_1 and U_2 are the evolution operators corresponding to the spin's passage through the magnetic field and the SG region, respectively.

Notably, the reliable projections E_1 and E_2 defined here are entirely independent of the magnetic field being measured. That is, these reliable projections do not contain any information regarding the physical quantity being assessed. Instead, they are solely related to the apparatus itself. By using these projections to characterize the apparatus's reliability, we can avoid the need for an external reference value to compare with the apparatus's readings, thereby eliminating the need for a standard reference scale.

Assuming that the target magnetic field and the SG region are sufficiently separated, one can independently calculate the evolution of the two processes: (1) scattering in the magnetic field and (2) evolution in the SG region. This evokes a surrogate model for the system described by equation (15) as follows.

4.2.1. Scattering in magnetic field. Consider a one-dimensional wave packet scattering problem in the far-field regime, as sketched in step 2 of figure 4. The Hamiltonian is given by

$$H_1 = \frac{p^2}{2m} + \Sigma_1(x) B_x \sigma_x. \quad (21)$$

It can be seen that the magnetic field only affects the spin and the coordinate in the x -space, while the wave function in the z -direction just diffuses. By decomposing the initial spin into $|\uparrow\rangle = (|+\rangle + |-\rangle)/\sqrt{2}$, we can discuss it in terms of potential barriers (+) and wells (-), that is,

$$H_1^{(\pm)} = \frac{p^2}{2m} \pm \Sigma_1(x) B_x. \quad (22)$$

For $|\pm\rangle$, the corresponding transmission and reflection coefficients can be determined as follows:

$$T^{(\pm)} = \frac{4k_0 q_{(\pm)} e^{i(q_{(\pm)} - k_0)a}}{(k_0 + q_{(\pm)})^2 - (k_0 - q_{(\pm)})^2 e^{2iq_{(\pm)}a}},$$

$$R^{(\pm)} = \frac{(k_0^2 - q_{(\pm)}^2)(1 - e^{2iq_{(\pm)}a})}{(k_0 + q_{(\pm)})^2 - (k_0 - q_{(\pm)})^2 e^{2iq_{(\pm)}a}}, \quad (23)$$

where $q_{(\pm)} = \sqrt{2m(E \mp B_x)/\hbar^2}$ and $E = k_0^2/2m$.

The state after evolution under the Hamiltonian H_1 becomes:

$$U_1 |\Psi_0\rangle = e^{-iH_1 t_1/\hbar} |\Psi_0\rangle$$

$$= \begin{cases} \frac{1}{\sqrt{2}} (R^{(+)}|+\rangle + R^{(-)}|-\rangle) \otimes |\psi_{x0,-}\rangle \otimes |\psi_{z1}\rangle, & x < 0 \\ \frac{1}{\sqrt{2}} (T^{(+)}|+\rangle + T^{(-)}|-\rangle) \otimes |\psi_{x0,+}\rangle \otimes |\psi_{z1}\rangle, & a < x \end{cases} \quad (24)$$

Here, $|\psi_{x0,\pm}\rangle$ represents Gaussian wave packets propagating in both positive and negative directions, as defined in appendix B. The wave function in the z -direction has propagated for a time t_1 , resulting in a Gaussian wave packet ψ_{z1} with a width of $\sigma' = \sigma^2(1 + i\hbar t_1/m\sigma^2)$. The detailed derivations of equations (23) and (24) can be found in appendix B.

4.2.2. Evolution in SG apparatus. The SG apparatus spatially separates particles based on their spin orientation using a non-uniform magnetic field. Here, a SG apparatus with a non-uniform magnetic field along the z -axis is considered, as illustrated in step 3 of figure 4. This setup effectively separates particles into spin-up and spin-down orientations along the z -axis.

The Hamiltonian of SG apparatus is written with the linear approximation

$$H_2 = \frac{p^2}{2m} - B(z) \sigma_z \approx \frac{p^2}{2m} - f z \sigma_z. \quad (25)$$

Denote the input state of the SG apparatus as

$$|\Psi_1\rangle = (c_1|\uparrow\rangle + c_2|\downarrow\rangle) \otimes |\psi_{z1}\rangle \otimes |\psi_{x1}\rangle. \quad (26)$$

After evolving for a time t_2 in the SG apparatus, the wave function become

$$U_2 |\Psi_1\rangle = e^{-iH_2 t_2/\hbar} |\Psi_1\rangle$$

$$= (c_1|\uparrow\rangle \otimes |\psi_{z2}^{(+)}\rangle + c_2|\downarrow\rangle \otimes |\psi_{z2}^{(-)}\rangle) \otimes |\psi_{x2}\rangle, \quad (27)$$

where

$$\psi_{z2}^{(\pm)}(z, t_2) = \left\langle z \left| \psi_{z2}^{(\pm)}(t_2) \right. \right\rangle$$

$$= \frac{\left(\frac{\sigma'^2}{2\pi}\right)^{1/4}}{\sqrt{\sigma'^2 + \frac{i\hbar t_2}{2m}}} \exp \left[-\frac{if^2 t_2^3}{6\hbar m} - \frac{\left(z \mp \frac{ft_2^2}{2m}\right)^2}{4\left(\sigma'^2 + \frac{i\hbar t_2}{2m}\right)} \pm if z t_2/\hbar \right], \quad (28)$$

and $|\psi_{x2}\rangle$ is the result of the free evolution of $|\psi_{x1}\rangle$. This can be obtained through Wei–Norman theory, i.e.

$$\exp \left[-i \left(\frac{p^2}{2m} \pm f z \right) t/\hbar \right]$$

$$= \exp \left[-\frac{itp^2}{2m\hbar} \mp \frac{ift^2 p}{2m\hbar} \right] \exp \left[\mp \frac{iftz}{\hbar} - \frac{z}{if^2 t^3} 6m\hbar \right]. \quad (29)$$

Therefore, the populations in the upper half-plane $\tilde{\alpha}$ and the lower half-plane $\tilde{\beta}$ of the SG apparatus are

$$\tilde{\alpha} = \int_0^\infty (|c_1 \psi_{z2}^{(+)}|^2 + |c_2 \psi_{z2}^{(-)}|^2) dz,$$

$$\tilde{\beta} = \int_{-\infty}^0 (|c_1 \psi_{z2}^{(+)}|^2 + |c_2 \psi_{z2}^{(-)}|^2) dz, \quad (30)$$

respectively, representing the apparatus's readings. From these readings, we can infer the magnitude of the magnetic field from equation (14), i.e.

$$\tilde{B} = \frac{k_0 \hbar}{am} \arctan \sqrt{\frac{\tilde{\beta}}{\tilde{\alpha}}}. \quad (31)$$

4.3. Reliability of the system

After analyzing the two evolution processes separately, the system's reliability can be determined using equation (20). It is important to note that the incident state in the SG region is given by

$$\begin{aligned} |\Psi_1\rangle &= E_1 U_1 |\Psi_0\rangle \\ &= \frac{1}{\sqrt{2}} \left(T^{(+)} |+\rangle + T^{(-)} |-\rangle \right) \otimes |\psi_{x0,+}\rangle \otimes |\psi_{z1}\rangle. \end{aligned} \quad (32)$$

Hence, the coefficients in equation (26) read

$$c_1 = \frac{1}{2} \left(T^{(+)} + T^{(-)} \right), \quad c_2 = \frac{1}{2} \left(T^{(+)} - T^{(-)} \right), \quad (33)$$

and $|\psi_{x1}\rangle = |\psi_{x0,+}\rangle$. The state after projection of E_2 is

$$\begin{aligned} |\Psi_2\rangle &\equiv E_2 U_2 |\Psi_1\rangle \\ &= \int_0^\infty c_1 \psi_z^{(+)}(z) |\uparrow\rangle \otimes |z\rangle dz \otimes \langle x | \psi_{x2} \rangle |x\rangle dx \\ &\quad + \int_{-\infty}^0 c_2 \psi_z^{(-)}(z) |\downarrow\rangle \otimes |z\rangle dz \otimes \langle x | \psi_{x2} \rangle |x\rangle dx. \end{aligned} \quad (34)$$

The reliability of the system is

$$\begin{aligned} R &= \text{Tr} [|\Psi_2\rangle \langle \Psi_2|] \\ &= \int_0^\infty |c_1 \psi_z^{(+)}(z)|^2 dz + \int_{-\infty}^0 |c_2 \psi_z^{(-)}(z)|^2 dz. \end{aligned} \quad (35)$$

Given the magnetic field to be measured, there are two adjustable parameters in the apparatus: the incident momentum k_0 of the wave packet and the length b of the SG region. These parameters determine the evolution times of the wave packet in the magnetic field and SG apparatus, denoted as $t_1 = am/k_0$ and $t_2 = bm/k_0$ respectively. Based on these times, the reliability of the measurement apparatus R can be assessed, as shown in figure 5. Systematic error is defined as $\delta B_x = \tilde{B}_x - B_x$. When reliability is high and errors are minimal, $1 - \text{reliability}$ exhibits a similar functional trend as the error, as shown in figure 6. In this regime, reliability can accurately characterize the systematic error.

To determine the region where reliability is applicable, specifically where it can characterize systematic error, we analyze the derivative of δB_x ,

$$\frac{d}{dB_x} \delta B_x = \frac{k_0 \hbar}{am} \sqrt{\frac{\tilde{\beta}}{\tilde{\alpha}}} \frac{(\tilde{\alpha} \tilde{\beta}' - \tilde{\beta} \tilde{\alpha}')}{2 \tilde{\beta} (\tilde{\beta} + \tilde{\alpha})} - 1. \quad (36)$$

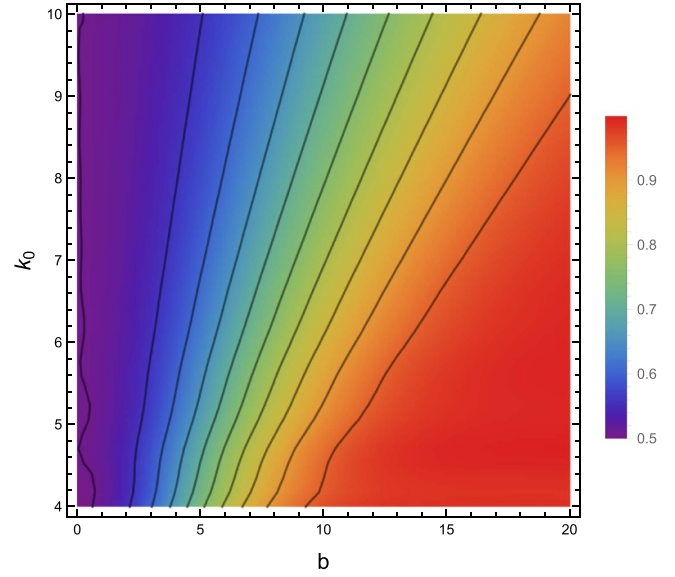


Figure 5. Reliability of the system. The black lines represent contour lines, and their curvature is attributed to resonant tunneling occurring during the scattering process. Parameters: $\hbar = 1$, $a = 3$, $m = 1$, $\sigma = 0.5$, $f = 1$, $B_x = 2$.

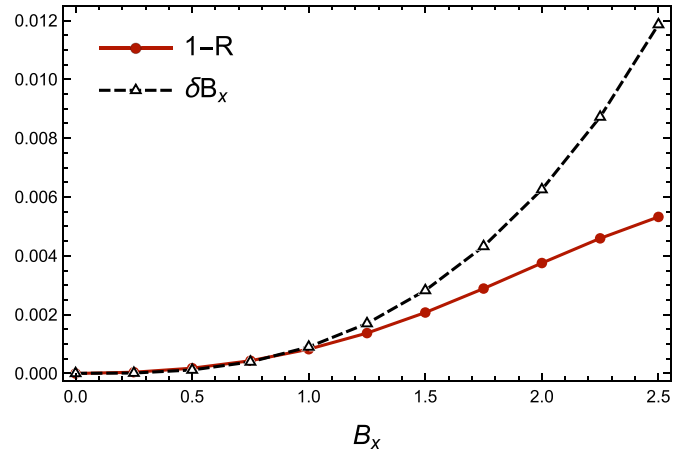


Figure 6. Reliability and error. $b = 35$, $k_0 = 5$.

As $B_x \rightarrow 0$ and $b \rightarrow \infty$, we expand the first term of the above equation and retain terms up to the first order

$$\sqrt{\frac{\tilde{\beta}}{\tilde{\alpha}}} \frac{(\tilde{\alpha} \tilde{\beta}' - \tilde{\beta} \tilde{\alpha}')}{2 \tilde{\beta} (\tilde{\beta} + \tilde{\alpha})} \approx \frac{B_x}{\sqrt{\text{Erf}(b/b_0) + B_x^2}}. \quad (37)$$

For a given b , the minimum magnetic field at which reliability is applicable is $B_{\min} \sim \sqrt{\text{Erf}(b/b_0)}$, where $b_0 = \sqrt{2\hbar k_0 / f m \sigma'}$ is the characterized length of the system. When b is sufficiently large, $B_{\min} \rightarrow 0$ can be considered negligible.

In the end, we validate the relationship derived in equation (1). When the system is nearly ideal, the relationship among reliability, sensitivity, and error is observed to be linear, as illustrated in figure 7. Here, it can be observed that the proportionality coefficient is independent of the magnetic field being measured.

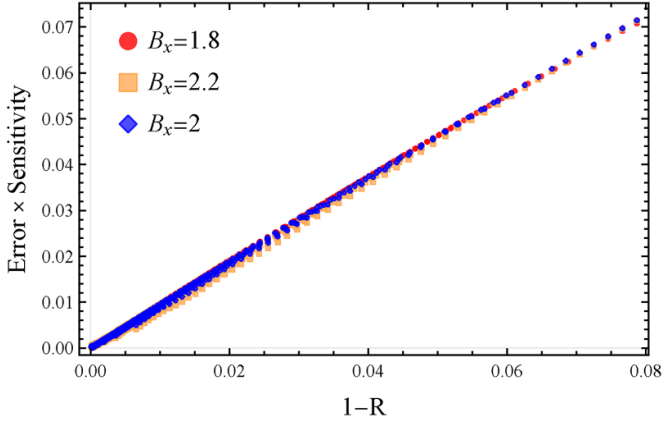


Figure 7. When the apparatus is near-ideal, the relationship among $1 - \text{reliability}$, sensitivity, and error is governed by equation (1). Parameters: $b \in [30, 50]$, $k_0 \in [10, 15]$.

5. Conclusion and discussion

In this paper, we propose a general relation among reliability, sensitivity, and error of measurement apparatus at first, as shown in equation (1). Then, with the definition of quantum reliability, as outlined in [28], we demonstrate this relationship through a specific quantum sensing model. We consider a specific quantum sensing process in which a spin is employed as a sensor to detect a magnetic field. The spin state is then read out using a SG apparatus, allowing us to infer the magnitude of the magnetic field. In this process, spins scatter after passing through the magnetic field to be measured, and the SG apparatus may not perfectly separate the spin wave packets, leading to systematic errors. Through the analysis of quantum reliability, we verify the above argument; thus, quantum reliability could be used to characterize the systematic error of the quantum sensing process. Additionally, we provide the parameter range within which this characterization is applicable.

In deriving the relationship expressed in equation (1), we considered only the first-order term in the expansion of equation (6). However, when the first-order term is not dominant, equation (1) no longer holds. For example, in this particular case, as B_x approaches zero, $dM/dB_x \rightarrow 0$. As a result, the second-order term $d^2M/dB_x^2 \times \delta^2 B_x$ is dominant. This implies the linear relationship between $1 - R$ and $\text{Error} \times \text{Sensitivity}$ breaks down, and is replaced by $\text{Error} \propto (1 - R)^{1/2}$, as illustrated in figure 8. Besides, for apparatuses reliant on highly non-linear behavior, such as criticality-enhanced quantum sensors [31–35], whether this relationship holds requires further study. Additional investigations are required to assess the reliability of these systems. Another pertinent issue in quantum reliability, warranting further study, is the inverse problem addressed in this paper: specifically, the generation of suitable projection operators that can effectively characterize a quantum apparatus's operational efficacy.

This work opens a new avenue for the reliability analysis of quantum systems, representing a significant application of quantum reliability. We have analyzed the reliability of quantum sensing process by translating classical metrics used

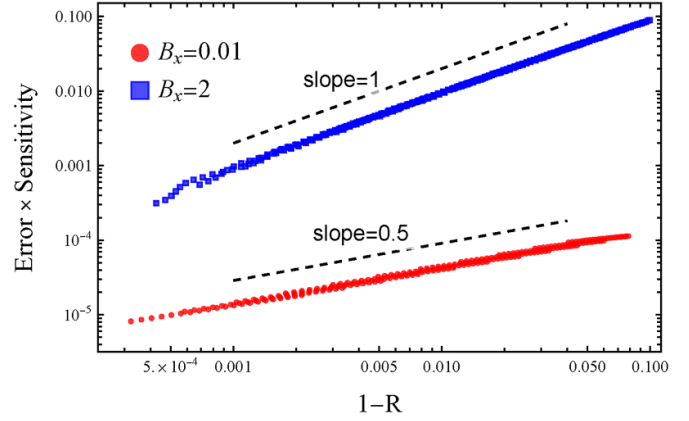


Figure 8. The scaling behavior differs when either the first-order or second-order terms dominate in equation (6). The blue line represents the scenario where the first-order terms prevail, adhering to the relationship described in equation (1). In contrast, the red line illustrates the case where the second-order terms are dominant. The sensitivity approaches zero, and $\delta Q \propto (1 - R)^{1/2}$. Parameters: $b \in [30, 50]$, $k_0 \in [13, 15]$.

to evaluate measurement apparatus, such as error, into the language of quantum reliability. In the absence of standard reference apparatus, this approach allows us to assess the accuracy of the apparatus through their reliability.

Acknowledgments

The authors appreciate Hui Dong for his fruitful discussions. This work was supported by the National Natural Science Foundation of China (NSFC) (Grant No. 12088101) and NSAF No. U2330401.

Appendix A. Equivalence between the overlap integral in SG experiment and the reliability projection in equation (19)

For a Stern–Gerlach apparatus, an inhomogeneous magnetic field spatially separates spins in different directions. Denote the two resulting wave packets as $\psi^+(z)$ and $\psi^-(z)$. Here, we do not require the specific form of the Hamiltonian; we begin by writing out the overlap integral of the two wave packets:

$$I_{\text{overlap}} = \left| \int_{-\infty}^{\infty} \psi^{+*}(z) \psi^-(z) dz \right|. \quad (\text{A1})$$

The reliability calculated through E_2 defined in equation (19) is

$$R_{\text{SG}} = \int_0^{\infty} |\psi^+(z)|^2 dz + \int_{-\infty}^0 |\psi^-(z)|^2 dz. \quad (\text{A2})$$

Considering a near-ideal scenario where the up and down wave packets are almost completely separated, we can extend the limits of integration in R_{SG} to encompass the entire space.

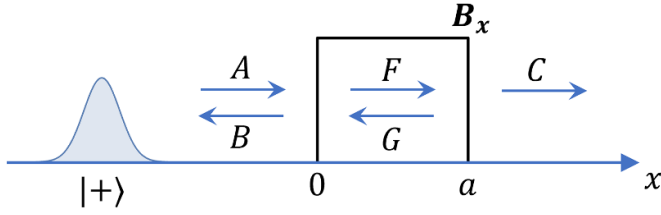


Figure 9. 1d far-filed scattering.

Applying the Cauchy–Schwarz inequality yields:

$$I_{\text{overlap}} \leq R_{\text{SG}}. \quad (\text{A3})$$

Considering that prolonged operation of the SG apparatus results in greater spatial separation of the two wave packets, we recognize that the overlap integral I_{overlap} and the reliability R_{SG} exhibit the same monotonic behavior. With the aforementioned inequality, we conclude that using R_{SG} to characterize the performance of the SG apparatus is equivalent to describing it in terms of the overlap integral.

Appendix B. 1D scattering in magnetic field

This appendix provides a detailed derivation of equations (23) and (24).

Taking the potential barrier(+) as an example (figure 9). For Hamiltonian $H^{(+)}$, we first solve its scattering state $\phi_k^{(+)} \equiv \langle x|k^{(+)}\rangle$, where $H^{(+)}|k^{(+)}\rangle = E_k|k^{(+)}\rangle$. Based on the Hamiltonians in different regions, the piecewise wave function can be expressed as:

- For $x < 0$, set $\phi_k^{(+)}(x) = Ae^{ikx} + Be^{-ikx}$, where $k = \sqrt{2mE_k/\hbar^2}$;
- For $0 < x < a$, set $\phi_k^{(+)}(x) = Fe^{iq_{(+)}x} + Ge^{-iq_{(+)}x}$, where $q_{(+)} = \sqrt{2m(E_k - B_x)/\hbar^2}$;
- For $x > a$, set $\phi_k^{(+)}(x) = Ce^{ikx}$.

According to the continuity conditions, i.e. the continuity of the wave function and its derivative at $x=0$ and $x=a$, we obtain the following four conditions:

$$\begin{aligned} T_k^{(+)} &\equiv \frac{C}{A} = \frac{4kq_{(+)}e^{i(q_{(+)}-k)a}}{(k+q_{(+)})^2 - (k-q_{(+)})^2 e^{2iq_{(+)}a}}, \\ R_k^{(+)} &\equiv \frac{B}{A} = \frac{(k^2 - q_{(+)}^2)(1 - e^{2iq_{(+)}a})}{(k+q_{(+)})^2 - (k-q_{(+)})^2 e^{2iq_{(+)}a}}, \\ M_{1k}^{(+)} &\equiv \frac{F}{A} = \frac{2k(k+q_{(+)})}{(k+q_{(+)})^2 - (k-q_{(+)})^2 e^{2iq_{(+)}a}}, \\ M_{1k}^{(+)} &\equiv \frac{F}{A} = \frac{2k(k+q_{(+)})}{(k+q_{(+)})^2 - (k-q_{(+)})^2 e^{2iq_{(+)}a}}, \\ M_{2k}^{(+)} &\equiv \frac{G}{A} = \frac{-2k(k-q_{(+)})e^{2iq_{(+)}a}}{(k+q_{(+)})^2 - (k-q_{(+)})^2 e^{2iq_{(+)}a}}. \end{aligned} \quad (\text{B1})$$

Thus, the scattering state can be obtained as:

$$\phi_k^{(+)}(x) = \begin{cases} e^{ikx} + R_k^{(+)}e^{-ikx}, & x < 0 \\ M_{1k}^{(+)}e^{iq_{(+)}x} + M_{2k}^{(+)}e^{-iq_{(+)}x}, & 0 < x < a \\ T_k^{(+)}e^{ikx}, & x > a \end{cases} \quad (\text{B2})$$

Here, $T_k^{(+)}$ and $R_k^{(+)}$ are referred to as the transmission coefficient and reflection coefficient, respectively. It is easy to check that $|T_k^{(+)}|^2 + |R_k^{(+)}|^2 = 1$.

Next, we decompose the initial state $|\psi_{x0}\rangle$ in terms of the scattering states $|k^{(+)}\rangle$ and demonstrate that the expansion coefficients in the scattering state basis are equivalent to those in the plane wave basis.

The expansion through plane wave reads

$$\psi_{x0}(x) = \frac{1}{\sqrt{2\pi}} \int_{-\infty}^{\infty} \varphi(k) e^{ikx} dk. \quad (\text{B3})$$

The expansion coefficients are

$$\begin{aligned} \varphi(k) &= \frac{1}{\sqrt{2\pi}} \int_{-\infty}^{\infty} \psi_{x0}(x) e^{-ikx} dx \\ &= \left(\frac{2\sigma^2}{\pi}\right)^{1/4} \exp[-ikx_0 - \sigma^2(k-k_0)]. \end{aligned} \quad (\text{B4})$$

The expansion in the scattering state reads

$$|\psi_{x0}\rangle = \frac{1}{\sqrt{2\pi}} \int_{-\infty}^{\infty} \tilde{\varphi}(k) |k^{(+)}\rangle dk, \quad (\text{B5})$$

where the expansion coefficients are

$$\begin{aligned} \tilde{\varphi}(k) &\equiv \frac{1}{\sqrt{2\pi}} \int_{-\infty}^{\infty} \langle k^{(+)}|x\rangle \langle x|\psi_{x0}\rangle dx \\ &= \frac{1}{\sqrt{2\pi}} \int_{-\infty}^{\infty} \phi_k^{(+)*}(x) \psi_{x0}(x) dx \\ &= \frac{1}{\sqrt{2\pi}} \int_{-\infty}^0 (e^{-ikx} + R_k^{(+)*} e^{ikx}) dx \\ &\quad + \frac{1}{\sqrt{2\pi}} \int_0^a (M_{1k}^{(+)*} e^{-iq_{(+)}x} + M_{2k}^{(+)*} e^{iq_{(+)}x}) dx \\ &\quad + \frac{1}{\sqrt{2\pi}} \int_a^{\infty} (T_k^{(+)*} e^{-ikx}) dx \\ &\approx \frac{1}{\sqrt{2\pi}} \int_{-\infty}^{\infty} (e^{-ikx} + R_k^{(+)*} e^{ikx}) dx \\ &\approx \varphi(k) + R_{k_0}^{(+)*} \varphi(-k) \approx \varphi(k). \end{aligned} \quad (\text{B6})$$

The approximate equality arises because the initial wave packet is localized far to the left, and its momentum is concentrated around $k_0 > 0$. At this point, the initial state can be expressed as an expansion in terms of the scattering states

$$\psi_{x0}(x) = \int_{-\infty}^{\infty} \varphi(k) \phi_k^{(+)}(x) dk. \quad (\text{B7})$$

We now calculate the time evolution of the wave function to determine the outgoing state. The wave function at time t reads

$$\psi_{x0}^{(+)}(x, t) = \int_{-\infty}^{\infty} \varphi(k) \phi_k^{(+)}(x) e^{-i\frac{\hbar k^2}{2m}t} dk \quad (\text{B8})$$

Substituting the scattering state from equation (B2) into the above expression, for $t \gg 0$, the parameter $e^{-i\frac{\hbar k^2}{2m}t}$ undergoes rapid oscillations, leading to the outgoing state given by

$$\psi_{x0}^{(+)}(x, t) = \begin{cases} R^{(+)}\psi_{x0,-}(x, t), & x < 0 \\ T^{(+)}\psi_{x0,+}(x, t), & x > 0 \end{cases} \quad (\text{B9})$$

where

$$\psi_{x0,\pm}(x, t) = \int_{-\infty}^{\infty} \varphi(k) \exp\left[\pm ikx - i\frac{\hbar k^2}{2m}t\right] dk \quad (\text{B10})$$


are the wave function transmission(+) and reflection(-), respectively.

Applying the same method to the $|-\rangle$ state, we obtain the total outgoing wave function in the magnetic field region as

$$U_1|\Psi_0\rangle = \begin{cases} \frac{1}{\sqrt{2}} \left(R^{(+)}|+\rangle + R^{(-)}|-\rangle \right) \otimes |\psi_{x0,-}\rangle \otimes |\psi_{z1}\rangle, & x < 0 \\ \frac{1}{\sqrt{2}} \left(T^{(+)}|+\rangle + T^{(-)}|-\rangle \right) \otimes |\psi_{x0,+}\rangle \otimes |\psi_{z1}\rangle, & x > 0 \end{cases} \quad (\text{B11})$$

Here, the wave function in the z -direction has propagated for a time t_1 , resulting in a Gaussian wave packet ψ_{z1} with a width of $\sigma' = \sigma^2(1 + i\hbar t_1/m\sigma^2)$.

ORCID iD

Lian-Xiang Cui (崔廉相)  <https://orcid.org/0009-0004-7890-6221>

References

- [1] Crocker L and Algina J 2008 *Introduction to Classical and Modern Test Theory* (Cengage Learning) (available at: <https://books.google.com/books?id=49tCGQAACAAJ>)
- [2] Kimberlin C L and Winterstein A G 2008 Validity and reliability of measurement instruments used in research *Am. J. Health-Syst. Pharm.* **65** 2276
- [3] Lachin J M 2004 The role of measurement reliability in clinical trials *Clin. Trials* **1** 553
- [4] Hibbert D B 2007 Systematic errors in analytical measurement results *J. Chromatogr. A* **1158** 25
- [5] Degen C L, Reinhard F and Cappellaro P 2017 Quantum sensing *Rev. Mod. Phys.* **89** 035002
- [6] Danilishin S L and Khalili F Y 2012 Quantum measurement theory in gravitational-wave detectors *Living Rev. Relativ.* **15** 1
- [7] Tse M et al 2019 Quantum-enhanced advanced ligo detectors in the era of gravitational-wave astronomy *Phys. Rev. Lett.* **123** 231107
- [8] Ebrahimi M, Nobahar E, Mohammadi R K, Noroozinejad Farsangi E, Noori M and Li S 2023 The influence of model and measurement uncertainties on damage detection of experimental structures through recursive algorithms *Reliab. Eng. Syst. Saf.* **239** 109531
- [9] Li Y, Gao H, Chen H, Liu C, Yang Z and Zio E 2024 Accelerated degradation testing for lifetime analysis considering random effects and the influence of stress and measurement errors *Reliab. Eng. Syst. Saf.* **247** 110101
- [10] Pulcini G 2016 A perturbed gamma process with statistically dependent measurement errors *Reliab. Eng. Syst. Saf.* **152** 296
- [11] Haim M, Jaeger M and Dov T 1997 An application of a Bayesian approach to the combination of measurements of different accuracies *Reliab. Eng. Syst. Saf.* **56** 1
- [12] Zhai Q, Ye Z-S, Yang J and Zhao Y 2016 Measurement errors in degradation-based burn-in *Reliab. Eng. Syst. Saf.* **150** 126
- [13] Pezzè L, Smerzi A, Oberthaler M K, Schmied R and Treutlein P 2018 Quantum metrology with nonclassical states of atomic ensembles *Rev. Mod. Phys.* **90** 035005
- [14] Braginsky V B and Khalili F Y 1996 Quantum nondemolition measurements: the route from toys to tools *Rev. Mod. Phys.* **68** 1
- [15] Safronova M S, Budker D, DeMille D, Kimball D F J, Derevianko A and Clark C W 2018 Search for new physics with atoms and molecules *Rev. Mod. Phys.* **90** 025008
- [16] Griffiths D J and Schroeter D F 2018 *Introduction to Quantum Mechanics* 3rd edn (Cambridge University Press)
- [17] Weinberg S 2015 *Lectures on Quantum Mechanics* 2nd edn (Cambridge University Press)
- [18] Horodecki R, Horodecki P, Horodecki M and Horodecki K 2009 Quantum entanglement *Rev. Mod. Phys.* **81** 865
- [19] Rabi I I, Zacharias J R, Millman S and Kusch P 1938 A new method of measuring nuclear magnetic moment *Phys. Rev.* **53** 318
- [20] Levitt M H 2008 *Spin Dynamics: Basics of Nuclear Magnetic Resonance* (Wiley)
- [21] Hämläinen M, Hari R, Ilmoniemi R J, Knuutila J and Lounasmaa O V 1993 Magnetoencephalography—theory, instrumentation and applications to noninvasive studies of the working human brain *Rev. Mod. Phys.* **65** 413
- [22] Du J, Shi F, Kong X, Jelezko F and Wrachtrup J 2024 Single-molecule scale magnetic resonance spectroscopy using quantum diamond sensors *Rev. Mod. Phys.* **96** 025001
- [23] Ludlow A D, Boyd M M, Ye J, Peik E and Schmidt P O 2015 Optical atomic clocks *Rev. Mod. Phys.* **87** 637
- [24] 2012 *International Vocabulary of Basic and General Terms in Metrology* (Joint Committee for Guides in Metrology)
- [25] 2008 *Guide to the Expression of Uncertainty in Measurement* (Joint Committee for Guides in Metrology)
- [26] American Society for Quality 2024 What is reliability? (available at: <https://asq.org/quality-resources/reliability>)
- [27] DiVincenzo D P 2000 The physical implementation of quantum computation *Fortschr. Phys.: Prog. Phys.* **48** 771
- [28] Cui L X, Du Y-M and Sun C P 2023 Quantum reliability *Phys. Rev. Lett.* **131** 160203
- [29] Griffiths R B 1984 Consistent histories and the interpretation of quantum mechanics *J. Stat. Phys.* **36** 219
- [30] Griffiths R B 2001 *Consistent Quantum Theory* (Cambridge University Press)
- [31] Quan H T, Song Z, Liu X F, Zanardi P and Sun C P 2006 Decay of loschmidt echo enhanced by quantum criticality *Phys. Rev. Lett.* **96** 140604
- [32] Zanardi P, Paris M G A and Venuti L C 2008 Quantum criticality as a resource for quantum estimation *Phys. Rev. A* **78** 042105
- [33] Fiderer L J and Braun D 2018 Quantum metrology with quantum-chaotic sensors *Nat. Commun.* **9** 1351
- [34] Frérot I and Roscilde T 2018 Quantum critical metrology *Phys. Rev. Lett.* **121** 020402
- [35] Yang L-P and Jacob Z 2019 Quantum critical detector: amplifying weak signals using discontinuous quantum phase transitions *Opt. Express* **8** 10482



Lian-Xiang Cui (崔康相) Graduated with a bachelor's degree in computational mathematics from Jilin University and currently a PhD student at the Beijing Computational Science Research Center. Research interests: quantum reliability, quantum information and quantum computing, complex systems.



Chang-Pu Sun (孙昌璞) Academician of the Chinese Academy of Sciences (CAS) and Fellow of the World Academy of Sciences for the advancement of science in developing countries (TWAS). Founding Dean of the Graduate School of China Academy of Engineering Physics (GSCAEP). He has long been engaged in research on quantum physics, mathematical physics, and the fundamental theory of quantum information. Currently, his work focuses on complex systems, energy physics, and reliability theory.



Yi-Mu Du (杜亦牧) Research associate professor in the Graduate School of China Academy of Engineering Physics. He received his PhD degree in theoretical physics from Zhejiang University in 2018. His current research interests include quantum reliability theory and percolation on complex networks.